[Frontiers in Bioscience E4, 1224-1236, January 1, 2012]

Different molecular targets of Icariin on bMSCs in CORT and OVX –rats

Qin Bian[1,2,3], Jian-hua Huang[2], Shu-fen Liu[1,3], You Ning[2], Zhu Yang[1,3], Yong-jian Zhao[1,3], Zi-yin Shen[2], Yong-jun Wang[1]

[1]Department of Orthopaedics and Traumatology, Longhua Hospital, Shanghai University of Traditional Chinese Medicine, No. 725 South Wan-ping Road, Shanghai, China, 200032, [2]Institute of integrated Traditional Chinese Medicine and Western Medicine, Huashan Hospital, Fudan University, No.12 Middle Wu lu mu qi Road, Shanghai, China, 200040, [3]Institute of Spine, Shanghai University of Traditional Chinese Medicine, No. 725 South Wan-ping Road, Shanghai, China, 200032

TABLE OF CONTENTS

1. ABSTRACT

Icariin (ICA) is an active component of *Herba Epimedium* effective in preventing osteoporosis. Bone mesenchymal stem cells (bMSCs) are an important target by which ICA promotes osteogenesis. However, its molecular mechanisms are poorly defined. In the present study, we induced osteoporosis in rats by corticosterone (CORT) and ovariectomy (OVX), treated both with ICA for 2 weeks or 3 months. As results, both models displayed bone loss tendency within 2 weeks and a significant bone loss after 3 months. ICA promoted bMSCs diffenentiation from CORT rat, and increased the secretion of osteocalcin, collagen I, runt-related transcription factor 2 in OVX model. Gene profile revealed a marked shift of gene expression by ICA, with much more significance in CORT rats. These potential molecular targets were involved in cell communication, adhesion, cycle and cytokines secretion. But very few genes overlapped in these two models, suggesting the effects and molecular mechanisms of ICA on osteoporosis might be pathogenesis-dependent. However, the Notch signaling pathway was common in both models, and should be paid close attention to for further study.

2. INTRODUCTION

Osteoporosis represents a major health problem, affecting more than 30% of women above 50 years old(1). Thus the basic research for osteoporosis is an active area, and it is necessary to identify new drugs for osteoporosis. *Herba Epimedium* is common used in the treatment of osteoporosis in China. It was found to prevent osteoporosis in both ovariectomy- (OVX) and glucocorticoid-induced rat models(2,3). More and more studies have confirmed Icariin (ICA), a flavonoid glycoside would be the principal component of Epimedium effective in promoting osteogenesis. It not only increased bone mass density (BMD) and biological strength *in vivo,* but also facilitated bone mesenchymal stem cells (BMSCs) proliferation and differentiation *in vitro*(4-6). Several reasons, including the extremely low cost, its high abundance in nature, a long-term and safe application of its original herbs, *Herba Epimedium*, make icariin appealing for bone regenerative medicine.

BMSCs may be an important cellular target through which ICA exerts its pro-osteogenetic effects. BMSCs are multipotent cells able to differentiate into

different distinct cell types including osteoblasts, adipocytes, and chondrocytes et al.(7). Studies concerning the isolation, growth, and differentiation of MSCs are of clinical interest because of their possible use in tissue engineering and in our understanding and treatment of osteoporosis. Studies showed that osteogenic differentiation by ICA *in vitro* was somewhat related to regulation of signaling molecules involving in a bone morphogenetic protein (BMP) and Runx2 signaling(8). Estrogen receptor(9), TGF and Wnt pathway might also be involved in the pro-osteogenic effect of ICA on bMSCs *in vitro*(10,11). However, the molecular targets of ICA, especially the *in vivo* action mechanisms are widely unknown.

In the present study, we observed the osteogenetic effect of ICA in two osteoporosis rats' models induced by CORT or OVX, and explored their potential molecular mechanism on bMSCs using stem cell microarray. We illustrated first the gene expression patterns induced by ICA *in vivo*. Our study would provide a basic evidence for further study of ICA molecular multitargets effects in the osteoporosis treatment.

3. MATERIALS AND METHODS

3.1. Preparation for drugs

Icariin (purity>98%, MW: 676.65) was purchased from You-si Biotech Co. (Shanghai, China). Icariin powder was ground and suspended into physiological saline to give a final concentration of 4mg/ml for experiment *in vivo* and *ex vivo*. The solutions of Icariin were prepared in dimethylsulfoxide (DMSO, Sigma, MO, USA) for experiment *in vitro*. The final concentration of DMSO used was 0.1%. Solutions of CORT (Merck KgaA, Darmstadt, Germany) were obtained in olive oil at a concentration of 20mg/ml.

3.2. Animals grouping and treatments

Two-month-old female Sprague-Dawley rats were provided by Shanghai laboratory animal centre (SCXK 2007-0005, Science and Technology Commission of Shanghai Municipality, Shanghai Animal Ethics Committee gave approval for the experimental research on animals). All rats were assigned into two experimental protocols. Rats in the first protocol were accepted a 2-week handling, and rats in the second protocol were accepted a 3-month handling. In the first protocol, Thirty-two rats were randomly divided into Normal, CORT, CORT+ICA and Normal+ICA groups. The rats in the CORT and CORT+ICA groups were subcutaneous injected with CORT once a day for fourteen days. The normal rats were given olive oil of equal dose. Other twenty-four rats were detected for OVX experiment: Sham group, OVX group and OVX+ICA group. ICA groups were intragastrically administered with Icariin at dose of 20mg/(kg·d) on five days before CORT-injection or OVX surgery. In the second protocol, every eight rats were assigned randomly into Control, CORT, CORT+ICA, Sham, OVX, OVX+ICA group. ICA groups were intragastrically administered with Icariin at dose of 20mg/(kg·d) on five days before CORT-injection or OVX surgery and lasted for 3 months.

3.3. Micro-CT Analysis

Analyses were performed using the uCT 80 radiograph Microtomograph (Scanco Medical AG, Switzerland), and associated 3DCalc, cone reconstruction and AVG model building software (HP, Japan). Lumbar spine specimens were fixed in 4% paraformaldehyde for 24h and washed with tap water for 2h, then examined. Their radiographs were obtained first, and L_4 vertebrates were chosen for fine scan. Only vertebrae were described for 3D model without showing adnexa such as transverse and spinous processes. A reconstruction of the bitmap data set was obtained and used to build the 3D model.

3.4. BMSCs culture and treatment

BMSCs were obtained from the bone marrow of the bilateral tibia and femur of rats on the 14th day after corticosterone-intervented or after OVX surgery. The marrow cavity was flushed with dulbecco modified eagle medium-high glucose (DMEM-HG) (Biowest, France) containing 10% fetal bovine serum (FBS), 1% penicillin-streptomycin (Gibico, USA). The cells of a rat were seeded into a 10 cm culture dish and incubated at 37°C in a 5% CO_2 humidified atmosphere. The medium was replaced on the 2nd and 5th day.

3.5. ALP staining

For the differentiation assay, BMSCs were cultured in the basal culture medium for 7 days. The cells were fixed with 10% formalin for 15 min, washed with PBS for three times, and stained with NBT-BCIP for 30 min at 37°C. A picture was taken using 450D cameras (Canon, Japan). Lyons blue represents the positive staining.

3.6. Immunohistological staining

Sections were incubated in 3% H_2O_2 to block endogenous peroxidase activity for 15 minutes, washed with PBS for 2 minutes, followed by a digestion with protease K for 10 minutes. Sections were blocked with 5% BSA in which the secondary antibody was produced, and then washed with PBS for 2 min 3 times. Specific primary mouse monoclonal antibodies against osteocalcin (1:100), Runx2 (3:500, Abcam Ltd. Cambridge, UK) were incubated overnight at 4°C. After extensive washing with PBS 2 min 3 times, the sections were incubated with the biotinylated anti-mouse-IgG for 15 min at 37°C followed by Streptavidin-HRP for 10 min at 37°C. Bound complexes were visualized using 3,3'-diaminobenzidine (DAB) reagent, counterstained with hematoxylin, dehydrated and mounted with gummi. L_4 and L_5 were examined. In immunofluorescence examination for Runx2, the goat anti-mouse-IgG-FITC (Southern Biotech, Birmingham, Alabama, USA) was incubated for 1h in dark room. After extensive washing with PBS three times for two minutes, fluorescence microscope was used for observation and photograph was taken within one hour to prevent fluorescent from decreasing.

3.7. Oligo GEArray experiments

We chose bMSCs of CORT and OVX rats at the end of 2 weeks for microarray profiling. Total RNA was

Table 1. Sequences of primers used in the real time RT-PCR

Genes	Forward and reverse primer	Product length(bp)
β -actin	F:5'CCTGTACGCCAACACAGTGC3' R:5'ATACTCCTGCTTGCTGATCC3'	211
Dll1	F:5'CAATGGAGGACGATGTTCAGATA3' R:5'GCACAGGTAAGAGTTGCCGAG3'	160
Mfng	F:5'GCTCCCTCCATTGTCTCCTCT3' R:5'TCAGGCAGTAGCATCCATCAT3'	103
Numbl	F:5'TGAGCCTACGGTTGAATGAGC3' R:5'GGCAGAAGTCCCTGTTGTGG3'	203
Adam17	F:5'AGTCTGCCTGGCTCATCTTT3' R:5'TTTCCTCCTTGGTCCTCATT3'	303

extracted from bMSCs after 7 days of culture with Trizol reagent (Invitrogen, USA). Agarose gel electrophoresis was used to check the quality of the RNA. The cRNA was labeled and synthesized with the TrueLabeling-AMP™ Liner RNA Amplification kit (SuperArray Frederick, MD, USA) and purified with the ArrayGrade™ cRNA Cleanup Kit (SuperArray). The membranes were hybridized in the GEAhyb Hybridization Solution (SuperArray) with 3-4 μg of cRNA probe and washed following the manufacturer's instructions. Signals were detected with the Chemiluminescent Detection Kit (SuperArray) and exposed to X-ray films. The clustering analysis was performed with R software version 2.11.1.

3.8. Real time RT-PCR detection

BMSCs were directly processed following RNA prep pure Cell Kit protocol. One microgram of total RNA was reversely transcribed using the Advantage RT-for-PCR kit (Qiagen, Valencia, CA) following the manufacturer's protocol. Freshly transcribed cDNA (1μl) was used for quantitative real-time PCR using SYBR Green (Bio-Bad, Hercules, CA) to monitor DNA synthesis using specific primers (Table 1) designed by TaKaRa Biotechnology Co. Ltd.. The PCR was carried out in RotorGene real-time DNA amplification system (Corbett Research, Sydney, Australia) using the following cycling protocol: a 95°C denaturation step for 3 min followed by 40 cycles of 95°C denaturation (15 s), 59-60°C annealing (20 s), and 72°C extension (20 s). Gene expression was normalized to the housekeeping gene β-actin. PCR products were subjected to a melting curve analysis, and the data were analyzed and quantified with the RotorGene6.0 analysis software.

3.9. Statistical analysis

The data is expressed as mean ± SE and statistical significance was calculated using One-Way ANOVA and analysis of variance by SPSS software (SPSS Inc, Chicago, USA). The significance level was defined as $p<0.05$. For microarray expression data analysis, the web-based DAVID DATABASE was used. Pathway analysis was a functional analysis mapping genes to KEGG pathways.

4. RESULTS

4.1. The micro-CT 3D morphometry for bone mass

The 3D morphometry showed no significant changes in bone mass such as BV/TV, Tb.Sp, Tb.Th, Tb.N, Conn D and Anistrophy in CORT treated rats for 2 weeks. In CORT treated rat model, ICA did not result in significant effects on bone mass. But we found that the reduction in BV/TV and Tb.Th and an increase in Conn D were observed in normal+ICA group rats (Figure 1A-B). In OVX rat osteoporosis model of 2 weeks, there was a significant decrease in BV/TV, and other indexes also displayed bone loss tendency though there was no statistical significance. After treatment by ICA for 2 weeks, all bone mass indicators showed improved tendency (Figure 1C-D). These results suggested a start of bone mass loss in both model rats, which would be partly prevented by ICA. In this study, the time of 2 weeks was not long enough to create osteoporosis evaluated by the morphometry data.

Next we extended the time window of CORT treatment or OVX to 3 months. As results, CORT rats showed decreased BV/TV, Tb.Th, Tb.N, Conn D, while increased Tb.Sp. After treatment by ICA, BV/TV, Tb.Sp, Tb.Th were significantly restored with decreased Tb.Sp. And in OVX rats, BV/TV, Tb.Th, Tb.N were significantly decreased while the Tb.Sp, and Conn D were significantly increased, indicating an impaired bone mass. After ICA treatment, the BV/TV, Tb.Sp, Tb.Th, Tb.N were all recovered (Figure 2A-B). In OVX rats, the Tb.Th was markedly increased, the Conn D decreased toward sham rats. ICA treatment also increased the Anistrophy of OVX rats (Figure C-D). These results showed that ICA possesses a time-dependent efficacy in preventing bone loss in CORT and OVX models.

4.2. The induction of differentiation by ICA on BMSCs

BMSC is considered as the original of osteoblast. A decline in bMSCs usually initiate bone loss in aging(12). ALP activity is an early indicator of bone formation, and commonly used in detection for bMSCs differentiation. In the present study, we found less ALP positive staining for bMSCs in CORT rats, demonstrating a reduction in osteoblast differentiation (Figure 3). The result was consistent with Weinstein's(13). ICA increased the ALP staining in bMSCs from CORT and Normal+CORT model rats. This suggested that ICA might raise the differentiation potency of bMSCs in both CORT and normal conditions, and the osteogenetic effect of ICA was not impairment-dependent.

In OVX model, we observed the expression of several osteogenic markers including osteocalcin (OC), collagen I (Col I), and Runx2 using immunostaining. The expression of OC, Col I and Runx2 all became weaker in OVX rats compared with those in the sham rats (Figure 4). ICA treatment significantly increased their expressions, suggesting a pro-osteogenesis of ICA in OVX model.

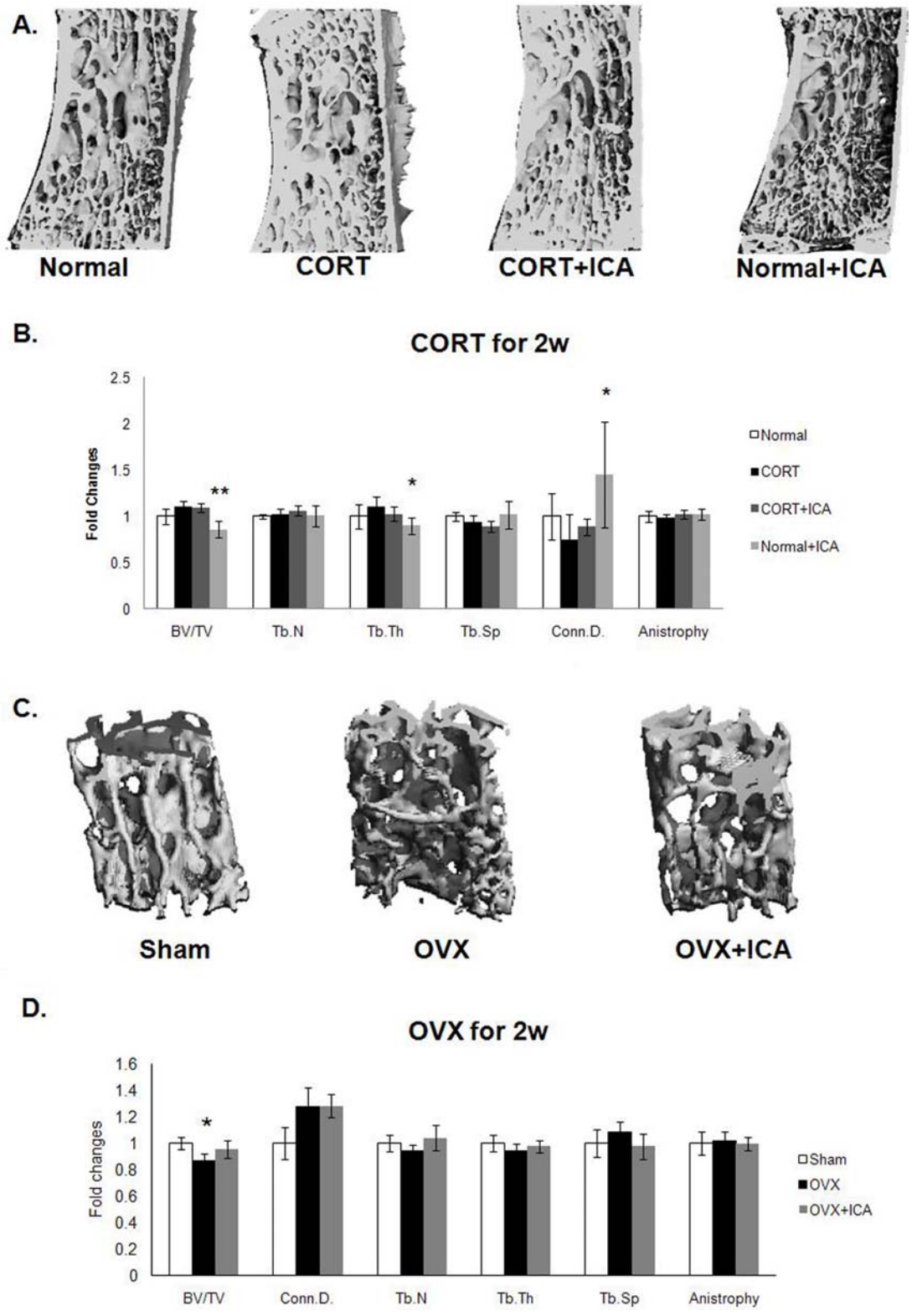

Figure 1. Micro-CT images and 3D morphometry of L_4 vertebrae in CORT (A,B) and OVX (C,D) rats treated with ICA. It showed a bone loss tendency with little statistical significance on the 2 weeks for the model creation. *p<0.05, **p<0.01 vs Normal or Control, $^{\#}p$<0.05, $^{\#\#}p$<0.01 vs CORT or OVX.

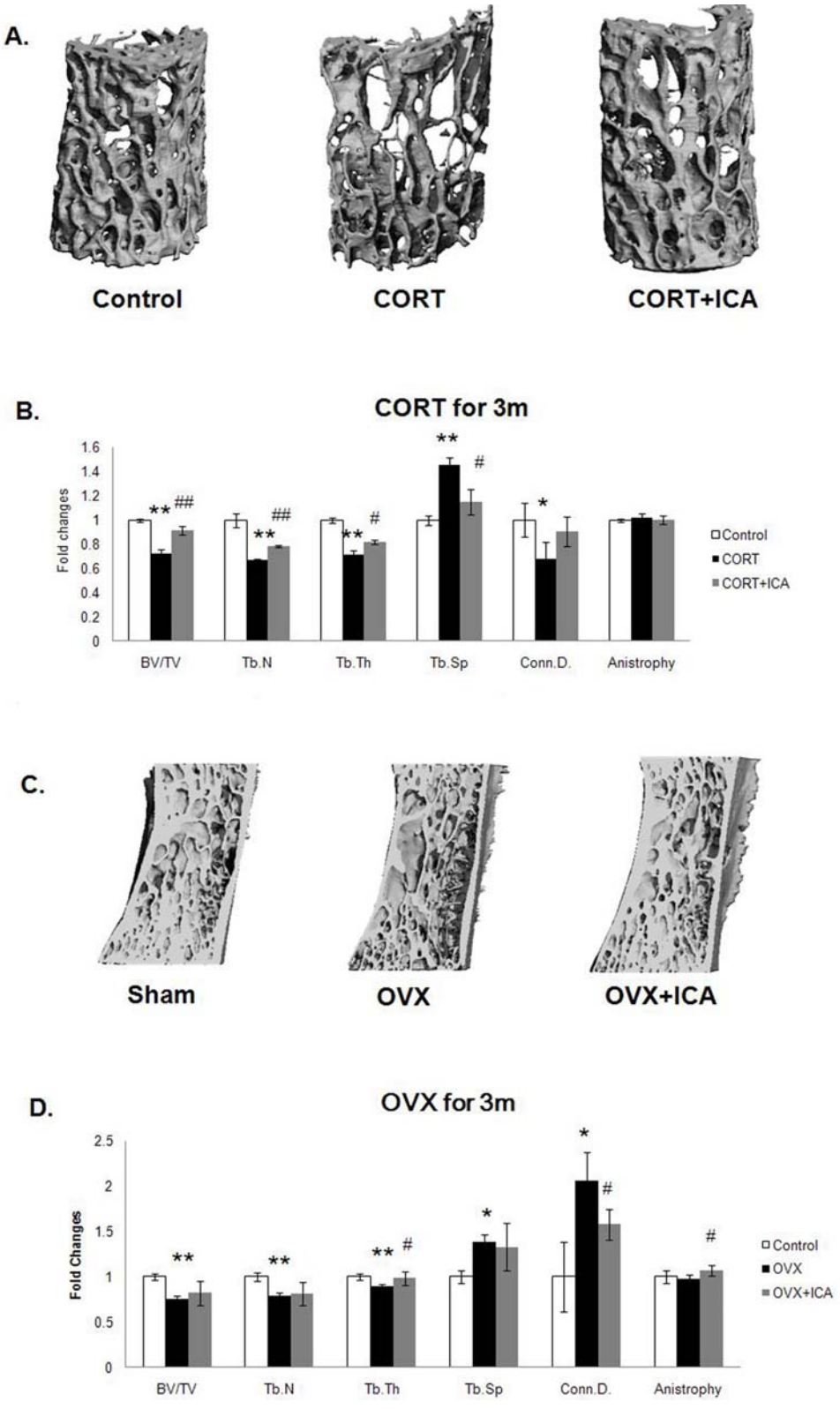

Figure 2. Micro-CT images and 3D morphometry of L_4 vertebrae in CORT (A,B) and OVX (C,D) rats treated with ICA. It showed a significant bone loss in model rats and ICA showed a significant efficacy in preventing loss of bone mass after 3 months of application. *p<0.05, **p<0.01 vs Normal or Control, $^{\#}p$<0.05, $^{\#\#}p$<0.01 vs CORT or OVX.

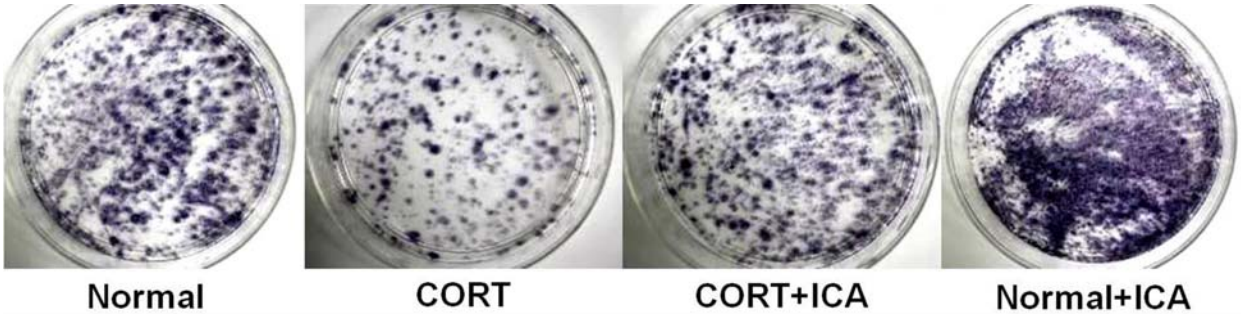

Figure 3. ALP staining for BMSCs cultured for seven days originated from Normal, CORT, CORT+ICA and Normal+ICA rats. The differentiation ability was raised by ICA in both normal and CORT condition.

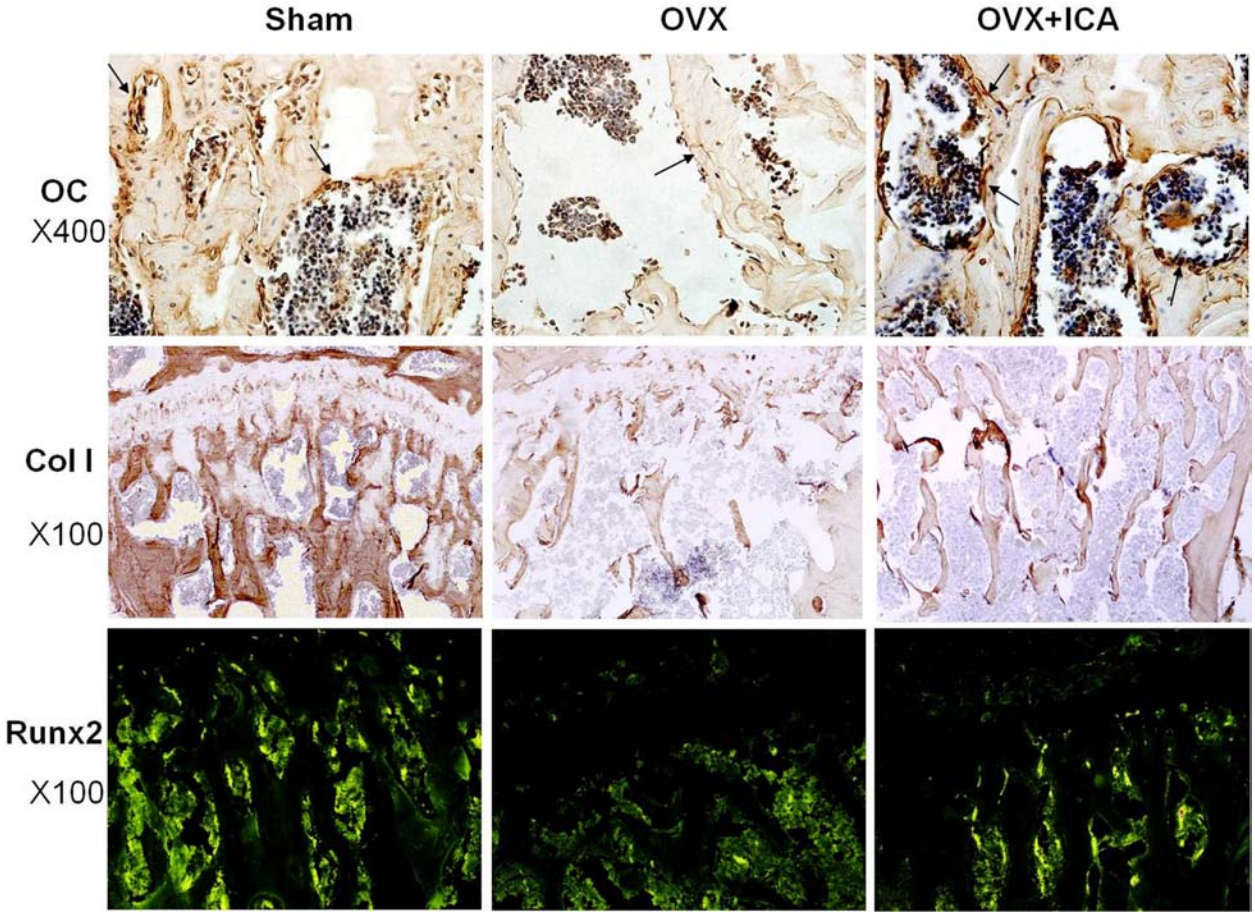

Figure 4. Osteogenesis indicated by immunostaining of OC, Col I and Runx2. OC was decreased in OVX rats, but strong positive staining was observed in OVX+ICA rats. Similar results were displayed for Col I and Runx2 staining. Results suggested an induction of osteogenesis by ICA.

4.3. Gene profile clustering revealed the differential effects of ICA on CORT or OVX -induced osteoporosis

To identify genes involved in the changes of bMSCs function in CORT- and OVX-induced osteoporosis, we used the Oligo GEArray Rat stem cell microarray that contains 256 genes related to the identification, growth and differentiation of stem cells. Results of the hierarchical clustering analysis were shown as a heatmap which can indicate the similarity in gene expression among either samples or genes. Here, we clustered seven samples including normal, CORT, CORT+ICA and normal+ICA groups, and sham, OVX, OVX+ICA groups. The samples fell into two major classes shown by the two branches of the dendrogram at the top of Figure 5. Interestingly, the classification exactly corresponded to the experimental grouping, the normal, CORT, CORT+ICA and normal +ICA in a dendrogram, the sham, OVX, OVX+ICA were in the other (Figure 5), suggesting a reliability of our gene expression measurement. According to the clustering, we also observed CORT treatment caused much greater gene

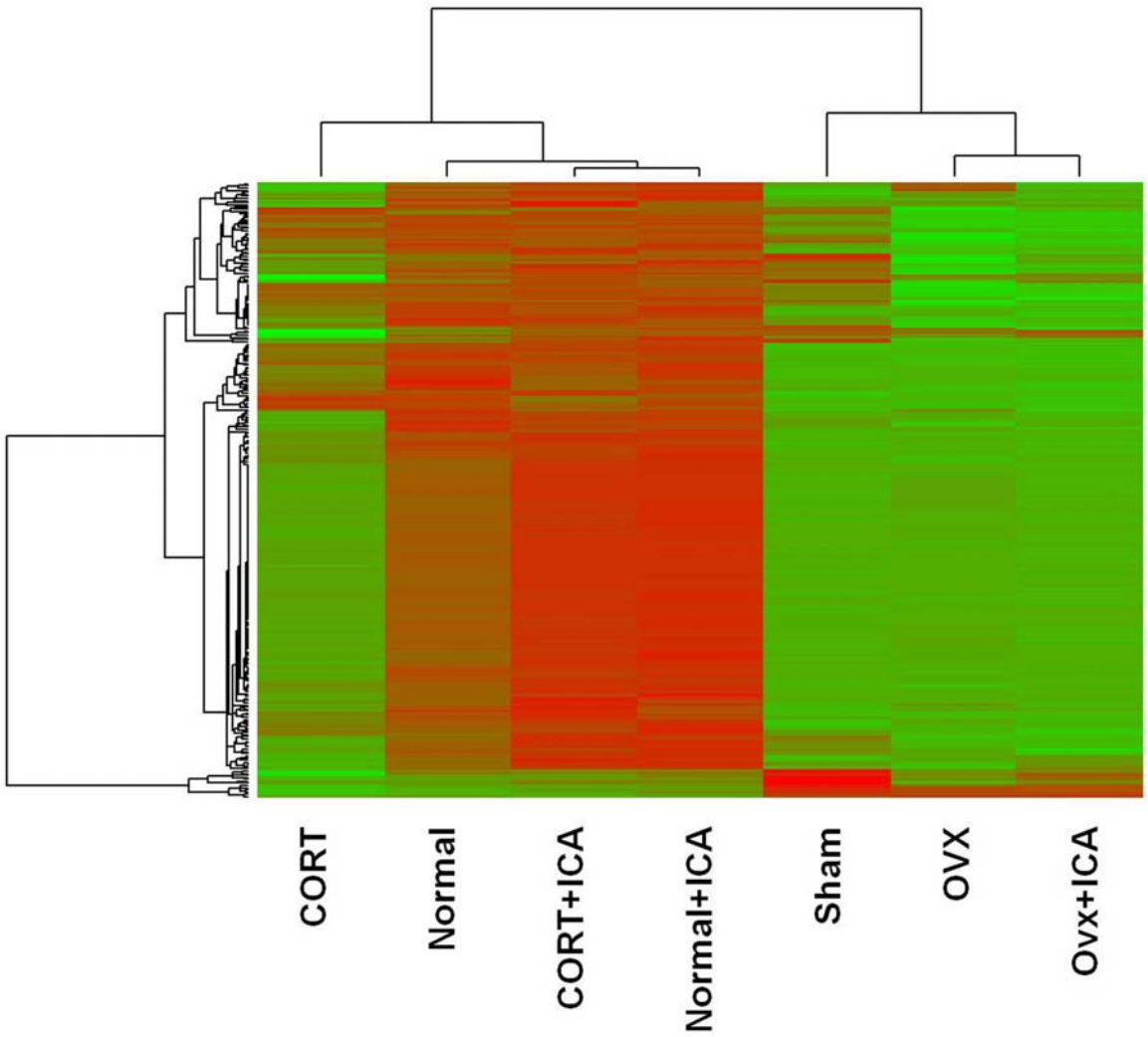

Figure 5. The hierarchical clustering of seven samples including Normal, CORT, CORT+ICA and Normal+ICA groups, and Sham, OVX, OVX+ICA groups on 256 genes. The samples fell into two major classes corresponding to CORT- or OVX-induced osteoporosis model. The results clearly showed ICA treatment in CORT rats shifted the gene expression profile toward normal rats.

expression changes in CORT model than in OVX–osteoporosis model. This was shown by greater color contrast in Figure 5. Further, the normal, normal+ICA, and CORT+ICA group became close together, but separated from model rats, the CORT group. This result indicated that ICA reversed the gene expression toward the normal rats. In sham, OVX, OVX+ICA group, ICA also reversed some genes expression (OVX vs. OVX+ICA), but the overall gene expressions remain closer to model rats, the OVX group.

4.4. The common and differential gene expression patterns caused by ICA in CORT or OVX -induced osteoporosis

We compared the expressed gene profile in five pairs of groups: between CORT and normal, ICA and CORT, normal+ICA and Normal, OVX and Sham, OVX+ICA and OVX. Differentially expressed genes (fold-changes >2.0 or <0.5) were shown in Table 2-6. Next, we identified the reversed genes by ICA in respective osteoporosis model. Eleven genes were inversed by ICA in CORT rats (Figure 6). These genes involved in cell communication such as Gap junction membrane channel protein beta 2 (Gjb2), cell adhesion as Cdh1 (Cadherin 1), cell cycle as Cdkn2a (Cyclin-dependent kinase inhibitor 2A), cytokines and their receptors participating in osteogenesis such as Bmp10 (Bone morphogenetic protein 10), Bmpr1a (Bone morphogenetic protein receptor, type 1A), Fgf21 (Fibroblast growth factor 21) and Fgfr2 (Fibroblast growth factor receptor 2). In OVX rats, nine genes were retrieved by ICA (Figure 6) and their functions were similar to those in CORT rats: cell communication related gene Gja3, cell adhesion as Ncam1 (Neural cell adhesion molecule 1), cell cycle as Cdc2 (Cell division cycle 2), cytokines such as Fgf17 and Bmp6.

Table 2. Genes regulated in CORT rats. (CORT *vs* Normal group)

GeneBank	Symbol	Fold regulation	GeneBank	Symbol	Fold regulation
NM_031539	Cd8b	4.24	NM_031334	Cdh1	0.24
NM_032063	Dll1	2.49	NM_138889	Cdh13	0.45
NM_001004099	Gjb2	2.09	NM_053593	Cdk4	0.43
NM_178866	Igf1	3.35	NM_031550	Cdkn2a	0.29
NM_199498	Krt19	2.35	NM_130812	Cdkn2b	0.37
NM_020306	Adam17	0.18	NM_012929	Col2a1	0.4
NM_031006	Adar	0.24	NM_012846	Fgf1	0.5
NM_013059	Alpl	0.22	NM_022223	Fgf14	0.46
NM_031012	Anpep	0.39	NM_130752	Fgf21	0.26
NM_012499	Apc	0.35	NM_130751	Fgf22	0.43
NM_001014255	Aph1a	0.24	XM_341940	Fgfr2	0.44
XM_217185	Aph1b	0.39	XM_344570	Fgfr4	0.16
NM_001031824	Bmp10	0.31	XM_221874	Flt3	0.26
NM_013107	Bmp6	0.24	NM_024360	Hes1	0.37
XM_342591	Bmp7	0.41	NM_133287	Numb	0.23
NM_030849	Bmpr1a	0.23	XM_214030	Pdgfra	0.31
NM_001007148	Btrc	0.40	XM_224334	Piwil2	0.28
XM_236196	Cd3e	0.48	NM_053423	Tert	0.44
NM_012705	Cd4	0.18			

Table 3. Genes regulated by ICA in CORT rats. (CORT+ICA *vs* CORT group)

GeneBank	Symbol	Fold regulation	GeneBank	Symbol	Fold regulation
NM_020306	Adam17	4.35	NM_181081	Myst2	2.32
NM_031006	Adar	2.66	XM_224334	Piwil2	2.65
NM_013059	Alpl	2.19	NM_013124	Pparg	4.60
NM_001031824	Bmp10	2.41	NM_053423	Tert	2.34
NM_030849	Bmpr1a	4.73	XM_573559	Bmp2k	0.33
NM_001007148	Btrc	3.48	XM_236415	Bmp5	0.36
XM_217136	Cd3g	2.64	NM_022177	Cxcl12	0.43
NM_031334	Cdh1	6.62	NM_032063	Dll1	0.24
NM_031550	Cdkn2a	3.42	NM_131908	Fgf6	0.48
NM_022205	Cxcr4	3.41	XM_001081521	Gja7	0.48
NM_130752	Fgf21	5.42	NM_017251	Gjb1	0.5
XM_341940	Fgfr2	3.17	NM_001004099	Gjb2	0.44
NM_022219	Fut4	2.12	NM_053984	Gjb4	0.43
NM_021266	Fzd1	2.14	NM_032080	Gsk3b	0.43
NM_001109607	Hint1	2.41	XM_344122	RGD1561440	0.46
NM_017339	Isl1	2.05	NM_176079	Myod1	0.48
NM_022264	Kit	4.53	NM_001009178	Pou5f1	0.41
XM_574919	Sox2	2.88	NM_013141	Ppard	0.35
NM_001109976	Map3k7ip1	2.25	NM_139254	Tubb3	0.45

Table 4. Genes regulated by ICA in Normal rats. (Normal+ICA *vs* Normal group)

GeneBank	Symbol	Fold regulation	GeneBank	Symbol	Fold regulation
NM_012924	Cd44	2.19	NM_138889	Cdh13	0.21
NM_031539	Cd8b	2.98	XM_001061943	Cdh4	0.49
NM_022219	Fut4	2.21	NM_130812	Cdkn2b	0.36
NM_021266	Fzd1	2.08	XM_344570	Fgfr4	0.16
NM_024360	Hes1	2.06	XM_221874	Flt3	0.44
NM_001109607	Hint1	2.33	NM_021654	Gja4	0.34
NM_133393	Lfng	2.16	XM_221997	Gjc3	0
XM_346070	RGD1565100	2.03	NM_022180	Hnf4a	0.43
NM_001031824	Bmp10	0.26	XM_225008	Myst3	0.31
NM_017178	Bmp2	0.47	NM_133287	Numb	0.35
NM_013107	Bmp6	0.18	XM_224334	Piwil2	0.25
XM_236196	Cd3e	0.48	XM_232595	Rbpsuh	0.43
NM_170789	Cd247	0.34	NM_139254	Tubb3	0.45
NM_012705	Cd4	0.21			

Furthermore, we compared the common and differential genes or signaling pathways responded to ICA. As a result, just two common genes were found, Adar and Map3k7ip, suggesting the most molecular response to ICA in different model was divergent. The common signaling pathway commonly responded to ICA was explored, we found that the effect of ICA in CORT condition are related to Notch signaling pathway for regulation of Delta (gene symbol: Dll1) and TACE (gene symbol: Adam17) (Figure 7-8)(14,15). Meanwhile, the Notch pathway related genes Mfng (Manic fringe homolog) and Numbl (Numb like) were regulated by ICA in OVX-induced osteoporosis. The results indicated the importance of this pathway in ICA action (Figure 7-8).

5. DISCUSSION

The decrease of bone mass in osteoporosis is related to a disequilibrium between bone resorption by osteoclasts and osteogenesis by osteoblasts(16,17) . Glucocorticoids (GCs) are useful drugs for the treatment of various diseases, but their use for prolonged periods can

Table 5. Genes regulated in OVX rats. (OVX *vs* Sham group)

GeneBank	Symbol	Fold regulation	GeneBank	Symbol	Fold regulation
NM_013059	Alpl	2.49	NM_019147	Jag1	0.19
NM_001014255	Aph1a	2.67	NM_013062	Kdr	0.36
NM_017178	Bmp2	3.23	NM_001109976	Map3k7ip1	0.36
XM_341639	Cdh11	2.38	NM_001014035	Mef2a	0.33
XM_001053056	Col10a1	2.07	NM_199110	Mfng	0.04
NM_032063	Dll1	2.50	NM_012603	Myc	0.39
NM_019198	Fgf17	3.35	NM_176079	Myod1	0.38
NM_024376	Gja3	2.45	NM_001017378	Myst1	0.48
NM_013124	Pparg	2.54	NM_181081	Myst2	0.33
XM_217185	Aph1b	0.48	NM_031521	Ncam1	0.21
NM_013107	Bmp6	0.45	XM_341072	Ncor2	0.50
XM_235962	Bmper	0.45	NM_174864	Ncstn	0.37
NM_012705	Cd4	0.48	NM_012987	Nes	0.47
NM_019296	Cdc2	0.39	NM_001033888	Numbl	0.49
NM_031334	Cdh1	0.16	NM_030996	Oprs1	0.44
NM_053615	Csnk1a1	0.46	XM_224334	Piwil2	0.37
XM_001070652	Dtx2	0.45	XM_342223	Prkci	0.49
XM_341940	Fgfr2	0.34	NM_021751	Prom1	0.15
NM_172334	Fibp	0.29	XM_001062978	Ptprc	0.21
NM_022219	Fut4	0.26	NM_001008384	Rac2	0.18
NM_053388	Gjb6	0.26	NM_001007799	Cir	0.36
NM_032080	Gsk3b	0.34	XM_340999	Tfrc	0.15
NM_001025409	Hdac1	0.24	NM_012673	Thy1	0.48
NM_178866	Igf1	0.25	XM_235639	Wnt1	0.38

Table 6. Genes regulated by ICA in OVX rats. (OVX+ICA *vs* OVX group)

GeneBank	Symbol	Fold regulation	GeneBank	Symbol	Fold regulation
NM_031006	Adar	2.06	NM_138889	Cdh13	0.36
NM_022407	Aldh1a1	5.85	NM_130812	Cdkn2b	0.42
NM_013107	Bmp6	2.55	NM_022205	Cxcr4	0.26
NM_019296	Cdc2	2.79	NM_053666	Dll3	0.44
NM_207613	Cdh15	2.77	NM_001003959	Dnmt3b	0.48
NM_019147	Jag1	3.76	NM_019198	Fgf17	0.35
XM_227549	Mov10	2.36	NM_024375	Gdf10	0.48
NM_001109976	Map3k7ip1	2.06	NM_024376	Gja3	0.41
NM_199110	Mfng	8.40	NM_019280	Gja5	0.18
NM_031521	Ncam1	2.75	XM_001081521	Gja7	0.44
NM_001033888	Numbl	2.54	NM_017251	Gjb1	0.40
XM_001062978	Ptprc	2.19	NM_053984	Gjb4	0.30
NM_139082	Bambi	0.16	NM_013035	Snai2	0.28

cause severe side effects such as osteoporosis. Osteoporosis induced by GCs is attributed to both direct inhibition of osteoblasts and impacting osteoclastive resorptive activity by disrupting its cytoskeleton(18). In OVX rats, the osteoporosis also involves increased bone turn over and decreased bone genesis. Here, we observed a marked time-dependent improvement in bone mass by ICA. During 2 weeks of treatment by ICA, bone mass of either CORT rats or OVX rats only showed increased tendency. After treatment for 3 months by ICA, multiple indicators for bone mass were significantly improved. The ALP staining for the bMSCs *ex vivo* and immunohistological staining showed enhanced differentiation toward osteoblast in both models by ICA. In addition, in our gene expression profile analysis, a significant shift of gene expression toward normal rats occurred after treatment by ICA in both models. Our results suggested that ICA possesses pro-osteogenic effects through differentiation of BMSCs. Until now, most osteoporosis treatments target bone resorption by inhibiting osteoclasts formation and activity, only a few promote bone formation. So ICA has the potential as a therapeutical agent to mainly mobilize osteoblast activity.

In gene expression profiling studies, we found a plenty of interesting information on the underlying mechanisms of ICA acting on BMSCs. In this study, two rat osteoporosis model was used, the CORT and OVX rats. The gene expression analysis showed Icariin treatment clustered the CORT+ICA and normal rats together, and separated from CORT model, suggesting a strong reversion of gene expression induced by CORT. In the OVX model, the reversion by ICA is to a much less extent. In ALP staining, we found significant promoted positive staining in ICA treated CORT rats. The ALP staining on BMSCs from OVX rats was not increased by ICA, but ICA enhanced significantly the expression of several osteogenic markers such as OC, Col I and Runx2. These results together seem to support an effect of induction of differentiation on bMSCs by ICA, but the effect was stronger in CORT model.

Next, we compared the common and differential genes regulated by ICA in both models. There are only two overlapped genes regulated by ICA between two models. This indicates that the most of effects of ICA on osteoporosis were pathology-dependent. Why the molecular targets were so different in both models remains a charming question, and needed to be researched in future.

We noticed that notch pathway was commonly significantly regulated by ICA in both models. The Notch

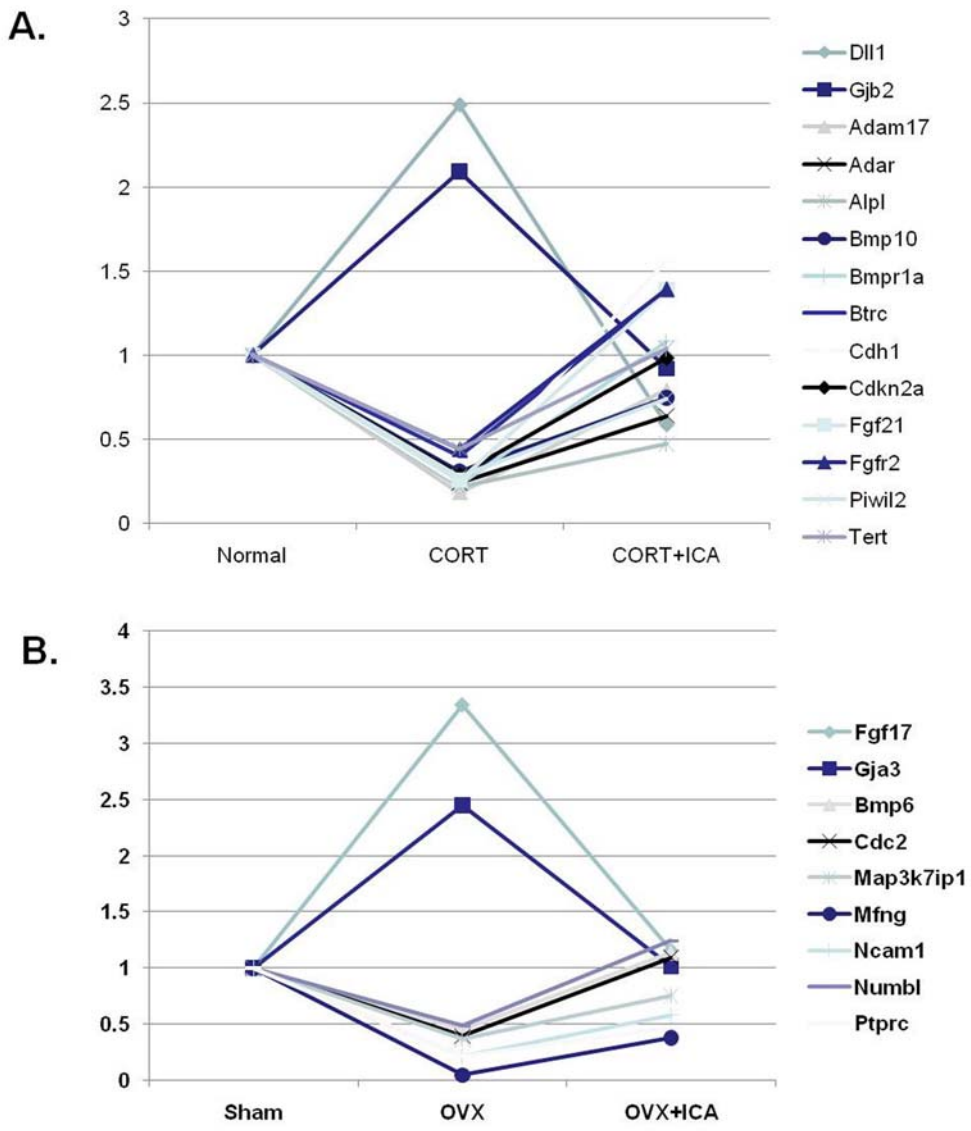

Figure 6. Genes retrieved by ICA. Eleven and nine genes were respectively inversed by ICA in CORT (A) and OVX (B) rats.

pathway is a highly conserved, ubiquitous signaling system that affects a variety of cell types and cellular processes(19). When specific ligands bind to notch, the intracellular domain of notch was released, and translocated to nucleus to interact with CSL [CBF1, Su(H), LAG1] transcription factors to regulate expression of Notch target genes(20). So far, a range of modulators of Notch pathway were found. Functional studies have now provided evidence that fringe proteins potentiate Notch signaling induced by Delta(21). The a disintegrin and metalloproteinase (ADAM) family member was reported to promote the ectodomain shedding of notch(22). Numb is a critical notch antagonist which can negatively modulate signaling pathway(23). In our study, the notch ligands Dll1 and Jag1 were up-regulated respectively. And the modulator of Adam17, Mfng, Numb1 were changed by ICA, suggesting the importance of this pathway in ICA action (Figure 5). To further validate the results from microarray, we tested these four genes in two models: bMSCs from OVX+ICA and CORT+ICA mice, by real time RT-PCT which repeated the microarray measurement. Although Notch pathway has been reported to play a key role in stem cells self-renewal and growth, and its component Adam17 or Dll1 mutant would cause bone loss in mice, the exact effects of gene Dll1, Adam17, Mfng and Numbl regulated in bone remodeling are less well understood (24-27).

Our results revealed the molecular targets of ICA were various in the treatment for osteoporosis of different pathogenesis. The function of these molecules would be involved in cell communication, cell adhesion, cell cycle and cytokines secretion. Furthermore, the effect of ICA on promoting osteogenesis might be related to Notch signaling

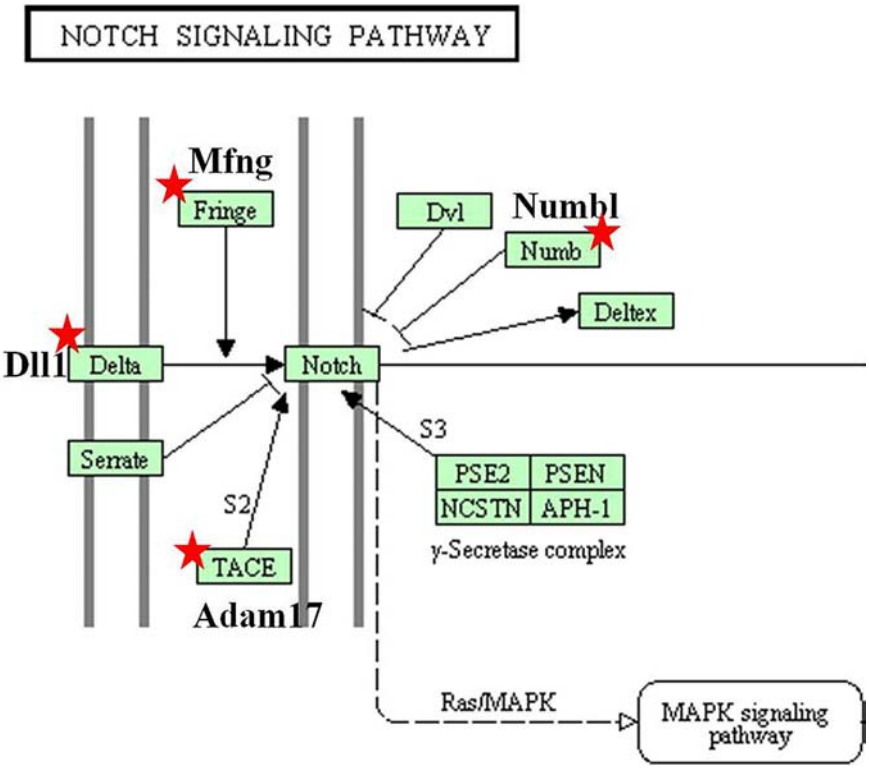

Figure 7. Notch signaling pathway based on KEGG analysis. Red stars represented proteins encoding by Dll1, Mfng, Numbl and Adam17, which were regulated by ICA in the microarray experiment.

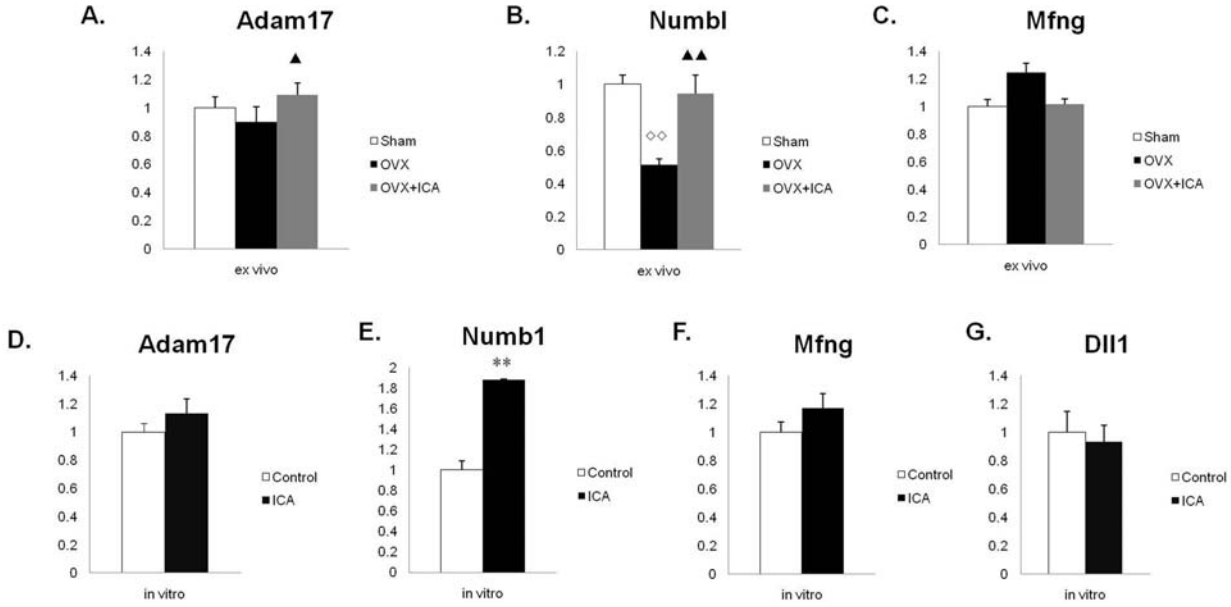

Figure 8. Dll1, Mfng, Numbl and Adam17 genes were validated by real time RT-PCR. Adam17 and Numbl mRNA up-regulated in bMSCs cultured with 10^{-6}M ICA *in vitro* and in bMSCs from OVX+ICA mice. There were no significant changes in Dll1 and Mfng gene levels in these two models. The columns represent the mean±SE. *p<0.05, **p<0.01 vs Controls, $^{▲}p$<0.05, $^{▲▲}p$<0.01 vs OVX, $^{◇◇}p$<0.01 vs Sham.

pathway, and Adam17 and Numbl molecules should be paid close attention to for further study.

6. ACKNOWLEDGMENTS

Qin Bian, Jian-hua Huang contributed equally to this paper. Zi-yin Shen and Yong-jun Wang were co-corresponding authors. We thank Professor Yi-ping Li, Department of Pathology, University of Alabama at Birmingham for support for the manuscript, and Xin-ming Zhang, Wei-hua Chen, Jian Ying, Bin Wu, Institute of integrated Traditional Chinese Medicine & Western Medicine, Huashan Hospital, Fudan University, Shanghai, China for technical guidance. This work was supported by National Basic Research Program in China (973 Plan, 2010CB530402, 2010CB530400), the International Cooperation Programs of National Natural Science Foundation of China (30710103904), the National Natural Foundation Committee (NSFC) of China key grant (30930111), the Project of National Natural Science Foundation of China (30701118, 81001526), Shanghai Science and Technology Development Funds(11QA1406600), Youth Health research project (2009Y092), Theories and therapies bones Province Key Laboratory of Ministry of Education, Shanghai University, Shanghai Education Commission Innovation Team Programme Section 6 (2009), Ministry of Education senior personnel items: Professor Changjiang Scholar Program (teaching people,2009,17).

7. REFERENCES

1. Keen, Richard: Osteoporosis: strategies for prevention and management. *Best Pract Res Clin Rheumatol* 21, 109-122 (2007)

2. Peng, Songlin; Xia, Renyun; Fang, Huang; Li, Feng; Chen, Anmin; Zhang, Ge; Qin, Ling: Effect of epimedium-derived phytoestrogen on bone turnover and bone microarchitecture in OVX-induced osteoporotic rats. *J Huazhong Univ Sci Technolog Med Sci* 28,167-170 (2008)

3. Du, J.; Ling, C. Q.; Chen, Y. A.: Effect of Herba Epimedil Brevicornus and prepared Radix Rehmannia on glucocorticoid receptor in glucocorticoid receptor down-regulated rats. *Zhongguo Zhong Xi Yi Jie He Za Zhi* 28, 64-67 (2008)

4. Nian, H.; Ma, M. H.; Nian, S. S.; Xu, L. L.: Antiosteoporotic activity of icariin in ovariectomized rats. *Phytomedicine* 16, 320-326 (2009)

5. Xiao, Q.; Chen, A.; Guo, F.: Effects of Icariin on expression of OPN mRNA and type I collagen in rat osteoblasts in vitro. J. Huazhong. *Univ Sci Technolog Med Sci* 25, 690-692 (2005)

6. Liu, H. J.; Wang, X. P.; Lin, J.; Yu, Y. C.; Jiang, X. Q.; Zhang, X. L.; Zhou, Z. T.; Zhang, W. D.: The effect of icariin and astragalosid I on the proliferation and differentiation of bone marrow stromal cells. *Zhong. Yao. Cai* 29, 1062-1065 (2006)

7. Baksh, D.; Song, L.; Tuan, R. S.: Adult mesenchymal stem cells: Characterization, differentiation, and application in cell and gene therapy. *J Cell Mol Med* 8, 301-316 (2004)

8. Zhao, Jiyuan; Ohba, Shinsuke; Shinkai, Masashige; Chung, Ung-il; Nagamune, Teruyuki; Icariin induces osteogenic differentiation in vitro in a BMP- and Runx2-dependent manner. *Biochem Biophys Res Commun* 369, 444-448 (2008)

9. Mok, Sao-Keng; Chen, Wen-Fang; Lai, Wan-Ping; Leung, Ping-Chung; Wang, Xin-Luan., Yao, Xin-Sheng; Wong, Man-Sau: Icariin protects against bone loss induced by oestrogen deficiency and activates oestrogen receptor-dependent osteoblastic functions in UMR 106 cells. *Br J Pharmacol* 159, 939-949 (2010)

10. He, W.; Li, Z. L.; Cui, Y. L.; Yi, B.; Liang, C.; Wang, X. X.; Li, Y.; Wang, X.: Effect of icariin on the mRNA expressions of Cbfalpha1, BMP2, BMP4 in rat osteoblasts. *Beijing Da Xue Xue Bao* 41, 669-673 (2009)

11. Yin, X. X.; Chen, Z. Q.; Dang, G. T.; Ma, Q. J.; Liu, Z. J.: Effects of Epimedium pubescens icariine on proliferation and differentiation of human osteoblasts. Zhongguo Zhong Yao Za Zhi 30, 289-291 (2005)

12. Zhang, Weixi; Ou, Guomin; Hamrick, Mark; Hill, William; Borke, James; Wenger, Karl; Chutkan, Norman; Yu, Jack; Mi, Qing-Sheng; Isales, Carlos M.; Shi, Xing-Ming; Age-related changes in the osteogenic differentiation potential of mouse bone marrow stromal cells. *J Bone Miner Res* 23:1118-1128 (2008)

13. Weinstein, R. S.; Jilka, R. L.; Parfitt, A. M.; Manolagas, S. C.: Inhibition of osteoblastogenesis and promotion of apoptosis of osteoblasts and osteocytes by glucocorticoids: potential mechanisms of their deleterious effects on bone. *J Clin Invest* 102, 274-282 (1998)

14. Hsieh, C. L.; Kumar, N. M.; Gilula, N. B.; Francke, U.: Distribution of genes for gap junction membrane channel proteins on human and mouse chromosomes. *Somat Cell Mol Genet* 17, 191-200 (1991)

15. Delwig, A.; Rand, M. D.: Kuz and TACE can activate Notch independent of ligand. *Cell Mol Life Sci* 65, 2232-2243 (2008)

16. Rodan, Gideon A.; Martin, T. John; Therapeutic approaches to bone diseases. *Science* 289, 1508-1514 (2000)

17. Teitelbaum, Steven L.: Bone resorption by osteoclasts. *Science* 289,1504-1508 (2000)

18. Kim, Hyun-Ju: New understanding of glucocorticoid action in bone cells. *BMB Rep* 43,524-529 (2010)

19. Weinmaster, Gerry: The ins and outs of notch signaling. *Mol Cell Neurosci* 9, 91-102 (1997)

20. Mumm, Jeffrey S.; Schroeter, Eric H.; Saxena, Meera T.; Griesemer, Adam; Tian, Xiaolin; Pan, D.J.; Ray, William J.; Kopan, Raphael: A ligand-induced extracellular cleavage regulates gamma-secretase-like proteolytic activation of Notch1. *Mol Cell* 5, 197-206 (2000)

21. Moloney, Daniel J.; Panin, Vladislav M.; Johnston, Stuart H.; Chen Jihua; Shao, LI; Wilson, Richa; Wang, Yang; Stanley, Pamela; Irvine, Kenneth D.; Haltiwanger, Robert S.; Vogt, Thomas F.: Fringe is a glycosyltransferase that modifies Notch. *Nature* 406, 369-375 (2000)

22. Reiss, Karina; Saftig, Paul: The "a disintegrin and metalloprotease" (ADAM) family of sheddases: physiological and cellular functions. *Semin Cell Dev Biol* 20, 126-137 (2009)

23. Petersen, Petur .H.; Zou, Kaiyong; Krauss, Stefan; Zhong, Weimin: Continuing role for mouse Numb and Numbl in maintaining progenitor cells during cortical neurogenesis. *Nat Neurosci* 7, 803–811(2004)

24. Butler, Jason M.; Nolan, Daniel J.; Vertes, Eva L.; Varnum-Finney, Barbara; Kobayashi, Hideki; Hooper, Andrea T.; Seandel, Marco; Shido, Koji; White, Ian A.; Kobayashi, Mariko; Witte, Larry; May, Chad; Shawber, Carrie; Kimura, Yuki; Kitajewski, Jan; Rosenwaks, Zev; Bernstein, Irwin D., Rafii, Shahin: Endothelial cells are essential for the self-renewal and repopulation of Notch-dependent hematopoietic stem cells. *Cell Stem Cell* 6, 251-264 (2010)

25. Mareddy, Shobha; Dhaliwal, Navdeep; Crawford, Ross; Xiao, Yin: Stem cell-related gene expression in clonal populations of mesenchymal stromal cells from bone marrow. *Tissue Eng Part A* 16, 749-758 (2010)

26. Horiuchi, Keisuke; Kimura, Tokuhiro; Miyamoto, Takeshi; Miyamoto, Kana; Akiyama, Haruhiko; Takaishi, Hironari; Morioka, Hideo; Nakamura, Takashi; Okada, Yasunori; Blobel, Carl P.; Toyama, Yoshiaki: Conditional inactivation of TACE by a Sox9 promoter leads to osteoporosis and increased granulopoiesis via dysregulation of IL-17 and G-CSF. *J Immunol* 182, 2093-2101 (2009)

27. Rubio-Aliaga, Isabel; Przemeck, Gerhard K.H. ; Fuchs, Helmut; Gailus-Durner, Valerie; Adler, Thure; Hans, Wolfgang; Horsch, Marion; Rathkolb, Birgit; Rozman, Jan; Schrewe, Anja; Wagner, Sibylle; Hoelter, Sabine M; Becker, Lore; Klopstock, Thomas; Wurst, Wolfgang; Wolf, Eckhard; Klingenspor, Martin; Ivandic, Boris T. ; Busch, Dirk H. ; Beckers, Johannes; Hrabé de Angelis, Martin: Dll1 haploinsufficiency in adult mice leads to a complex phenotype affecting metabolic and immunological processes. *PLoS One* 4, e6054 (2009)

Abbreviations: ICA: Icariin, bMSCs: bone mesenchymal stem cells, CORT: corticosterone, OVX: ovariectomy, OC: osteocalcin, ALP: alkaline phosphatase, Col I: collagen I, Runx2: runt-related transcription factor 2, BMD: bone mass density, BV/TV: the ratio of bone volume to tissue volume, Conn D: connectivity density of trabeculae, Tb.N: trabecular number, Tb.Th: trabecular thickness, Tb.Sp: trabecular spaces, BMP: bone morphogenetic protein, DMSO: dimethylsulfoxide, Gjb2: Gap junction membrane channel protein beta 2, Cdh1: cadherin 1, Cdkn2a: Cyclin-dependent kinase inhibitor 2A, Bmpr1a: bone morphogenetic protein receptor, type 1A, Fgf21: fibroblast growth factor 21, Fgfr2: fibroblast growth factor receptor 2, Ncam1: Neural cell adhesion molecule 1, Cdc2: Cell division cycle 2, GCs: Glucocorticoids

Key Words: *Herba Epimedium*, Icariin, Stem Cell Microarray, Bone Mesenchymal Stem Cell, Osteoporosis

Send correspondence to: Yong-jun Wang, Department of Orthopaedics & Traumatology, Longhua Hospital, Shanghai University of Traditional Chinese Medicine, No. 725 South Wan-ping Road, Shanghai, China, 200032, Tel: 86-21-64385811, Fax: 86-21-64875390, E-mail: yjwang88@126.com

http://www.bioscience.org/current/vol4E.htm